Structure and Stability of Complex Coacervate Core Micelles with Lysozyme

Saskia Lindhoud,* Renko de Vries, Willem Norde, and Martien A. Cohen Stuart

Laboratory of Physical Chemistry and Colloid Science, Dreijenplein 6, 6703 HB Wageningen, The Netherlands

Received January 19, 2007; Revised Manuscript Received March 28, 2007

Encapsulation of enzymes by polymers is a promising method to influence their activity and stability. Here, we explore the use of complex coacervate core micelles for encapsulation of enzymes. The core of the micelles consists of negatively charged blocks of the diblock copolymer $PAA_{42}PAAm_{417}$ and the positively charged homopolymer $PDMAEMA_{150}$. For encapsulation, part of the positively charged homopolymer was replaced by the positively charged globular protein lysozyme. We have studied the formation, structure, and stability of the resulting micelles for three different mixing ratios of homopolymer and lysozyme: a system predominantly consisting of homopolymer, a system predominantly consisting of lysozyme, and a system where the molar ratio between the two positively charged molecules was almost one. We also studied complexes made of only lysozyme and $PAA_{42}PAAm_{417}$. Complex formation and the salt-induced disintegration of the complexes were studied using dynamic light-scattering titrations. Small-angle neutron scattering was used to investigate the structures of the cores. We found that micelles predominantly consisting of homopolymer are spherical but that complex coacervate core micelles predominantly consisting of lysozyme are nonspherical. The stability of the micelles containing a larger fraction of lysozyme is lower.

Introduction

Complex coacervates are viscous liquids consisting of oppositely charged macromolecules. The classical example is phase separation between gum arabic and gelatin at acidic conditions, studied by Bungenberg de Jong.[1] More recently, complex coacervation is gaining interest. Since biomacromolecules, such as DNA, proteins, and polysaccharides, often are charged, complex coacervation can be used to construct particles for encapsulation, targeting, and delivery of functional ingredients in food[2] and pharmaceutics.[3] Furthermore, in food science the influence of complex coacervation on the structure and texture of food[4−6] is studied.

Previously, we have investigated block copolymer micelles with cores consisting of complex coacervates. These consist of diblock copolymers having both an electroneutral hydrophilic and a charged block mixed with either oppositely charged homopolymer or diblock copolymer.[7−10] At equal charge ratios electrostatic complexes of finite size are obtained that are stabilized by a hydrophilic corona. We call these complexes complex coacervate core micelles.[11] Stable micelles are formed when the neutral block is 3 times longer than the charged block.[7] It has also been found that a minimum block length is required for the formation of the complexes. Micelles made of an oppositely charged homopolymer and diblock copolymer are more resistant against salt than micelles made of two oppositely charged diblock copolymers.[8] Other authors have studied similar polymer micelles and called them polyion complex micelles (PIC micelles)[12] or block ionomer complexes (BICs).[13]

Complex coacervate core micelles can be used for different applications. It has been found that they spontaneously adsorb on substrates[14] and therewith may give the substrate protein-resistant antifouling properties. Other applications can be the encapsulation of nanoparticles in the core of these micelles. There are already micellar aggregates available with "soft" nanoparticles such as DNA and proteins in the core[15−24] and with "hard" nanoparticles such as oxide nanoparticles.[25−28] We are interested in using these micelles primarily for encapsulating enzymes.

When using these complex coacervate core micelles to encapsulate enzymes, there are a number of potential difficulties. Because electrostatics, which includes electrostatic attraction and entropy gain due to counterion release, is the main driving force of complexation, pH and ionic strength influence the stability of the micelles. The pH can influence the electrostatic attraction since the charge on, for example, proteins and other (bio)polymers usually originates from dissociation or association with protons and therefore varies with pH. As electrostatic interactions are screened by low-molecular-weight electrolytes in solution, one has to think about "tricks" to make structures at physiological ionic strength stable. Enzymes, i.e., globular proteins, have a charge density that is much lower than the charge densities of the homopolymers and diblock copolymers used. Therefore the ionic strength at which these structures disintegrate is expected to be lower than that for micelles without proteins in the core. Kataoka et al. solved this problem by increasing the hydrophobic interactions[20] and by cross-linking[21,24] the core with gluteraldehyde.

We use a different approach. To regulate the number of enzyme molecules in the cores of the complex coacervate core micelles, we mix proteins with like-charged homopolymers and let this solution form a complex with oppositely charged diblock copolymers. By changing the ratio between protein and homopolymer we are able to control the number of enzyme molecules in the cores of the particles. This also results in micelles that are more stable against disintegration by increases in ionic strength.

* Author to whom correspondence should be addressed. Phone: (+31) (0)317 482 585. Fax: (+31) (0)317 483 777. E-mail: saskia.lindhoud@wur.nl.

10.1021/bm0700688 CCC: $37.00
Published on Web 05/27/2007

Chart 1. Structures of (a) PAA_nPAAm_m and (b) $PDMAEMA_n$

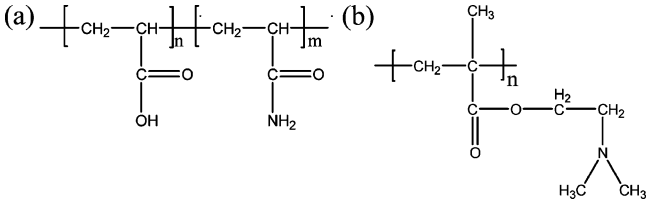

Our system consists of the negatively charged diblock copolymer $PAA_{42}PAAm_{417}$, the positively charged homopolymer $PDMAEMA_{150}$, and the positively charged globular protein lysozyme. We studied three systems with varying protein to homopolymer ratios. These systems are compared with the formation of complex coacervate core micelles without lysozyme, studied by Hofs et al.,[8] and complexes that are formed when lysozyme and $PAA_{42}PAAm_{417}$ are mixed.

We use dynamic light-scattering (DLS) titration measurements to study the formation of micelles. Starting with one of the charged species, we are able to study the existence and size of the complex coacervate core micelles as a function of the composition, expressed as a ratio between the concentrations of charges of one sign divided by the total concentration of charges. Dynamic light-scattering titrations can also be used to determine the ionic strength at which the complexes disintegrate. Dynamic light scattering only gives information about the hydrodynamic radius, which is mainly determined by the corona of the micelles. The corona thickness is larger than the double layer of the core, and therefore electrostatics does not influence particle diffusivity. To obtain information about the shape, structure, and the size of the core of the micelles, small-angle neutron-scattering (SANS) experiments were performed.

Experimental Section

Materials. Lysozyme (L6876) was purchased from Sigma and used without further purification. The poly(acrylic acid)-*block*-poly(acryl amide) ($PAA_{42}PAAm_{417}$, where the numbers refer to the number-averaged degree of polymerization) diblock copolymers were a gift from Rhodia, Auberville, France. For details of the synthesis see Taton et al.[29] The positively charged homopolymer used was poly(*N*,*N*-dimethylaminoethyl methacrylate) ($PDMAEMA_{150}$), purchased from Polymer Source, Inc., Canada.

Sample Preparation. Lysozyme was dissolved in demineralized water. The pH was adjusted to 6.5. Solutions were filtered (pore size, 0.1 μm), and the protein concentration was determined by UV (281.5 nm, 2.635 L g^{-1} cm^{-1}).[30] Diblock copolymer and homopolymer solutions were prepared by dissolving the molecules in demineralized water. The pH was adjusted to 6.5. The solutions were diluted to the desired concentration and a salt concentration of 5 mM NaCl. For the light-scattering titrations of the three-component systems, the solutions containing the like-charged molecules, i.e., lysozyme and PDMAEMA, were mixed first. This solution was always optically clear. There was no indication of the presence of aggregates in this solution during DLS measurements.

Dynamic Light-Scattering Titrations. Dynamic light scattering was performed with an ALV5000 multiple τ digital correlator and an argon ion laser with a wavelength of 514.5 nm. All measurements were performed at a scattering angle of 90°. The laser power used was 200 mW. Temperature was kept constant at 25 °C by means of a Haake C35 thermostat, providing an accuracy of ±0.1 °C. Titrations were performed using a Schott-Geräte computer-controlled titrations setup to control the addition of titrant, the cell stirring, and the delay times. The pH was recorded with a calibrated Mettler Toledo InLab pH electrode filled with a 3 M KCl solution.

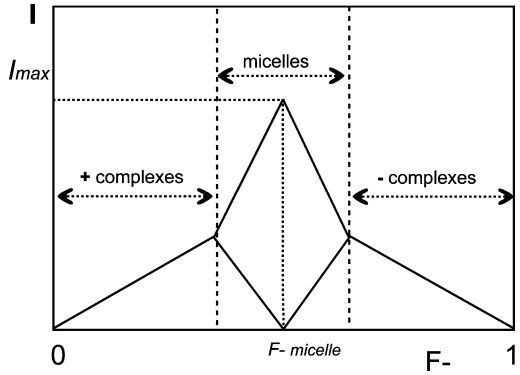

Figure 1. Schematical representation of the scattering intensity as function of composition (F^-) for complex coacervate core micelle formation studied by dynamic light scattering.

Two different types of titrations were performed: composition titrations and salt titrations. For the composition titrations the measurement cell contains macromolecules of the same charge sign. The titrant is a solution containing macromolecules of opposite charge. After every titration step the pH is measured and a light-scattering run is started; the typical number of light-scattering runs per titration step is five. The scattered intensity, the pH, and the hydrodynamic radius are recorded as a function of the composition F^- (eq 1)

$$F^- = 1 - F^+ = \frac{[-\text{ charges}]}{[+\text{ charges}] + [-\text{ charges}]} \qquad (1)$$

Effective average hydrodynamic radii of the complexes were determined by analyzing the autocorrelation function using the methods of cumulants and using the Stokes−Einstein equation for spherical particles. The composition was calculated in the following way: We know from proton titration curves that at pH 6.5 the net charges of the diblock copolymer and homopolymer are −29 and +105, respectively. But, because in these experiments pH is not fixed, for the calculation of F^-, we used the maximal amount of chargeable groups of the polymers. $PAA_{42}PAAm_{417}$ has 42 chargeable groups per molecule, and $PDMAEMA_{150}$ has 150 chargeable groups per molecule. For lysozyme we used +8 charges, based on a titration curve measured by Van der Veen et al.;[31] the number of net positive charges on the protein is almost constant in the pH interval between 6 and 8.5.

To determine the ionic strength at which the complex coacervate core micelles disintegrate we carried out light-scattering titrations with salt. For the salt titration solutions with a composition at $F^-_{micelle}$ (Figure 1) were prepared. The typical volume of these solutions was 9 mL. To these solutions a 4 M NaCl solution was titrated in steps of 10 or 20 μL. Both the intensity and the hydrodynamic radius were plotted as a function of the salt concentration. When the error in the average radius of five measurements was larger than 2 nm, the measurement is said to be unreliable, and its value is not plotted.

Small-Angle Neutron Scattering. Small-angle neutron-scattering measurements were performed at the time-of-flight instrument LOQ at ISIS (Rutherford Appleton Laboratory). The incident wavelengths are 2.2−10.0 Å, giving a scattering vector q between 0.008 and 0.287 $Å^{-1}$. For these measurements D_2O was used as a solvent, taking the difference in pH and pD into account.[32] All measurements were performed at 25 °C. Samples were prepared with a concentration of 10 g/L, having the solution composition $F^-_{micelle}$ (Figure 1). Solutions were kept in quartz cells with a path length of 5 mm. All samples were corrected for sample transmission, background scattering, and thickness. From the raw spectra absolute intensities were determined using a polymer standard (a solid blend of protonated and deuterated polystyrene with a known scattering cross-section), which was provided by ISIS. Small-angle neutron-scattering measurements were analyzed using the generalized indirect Fourier transformation (GIFT) method.

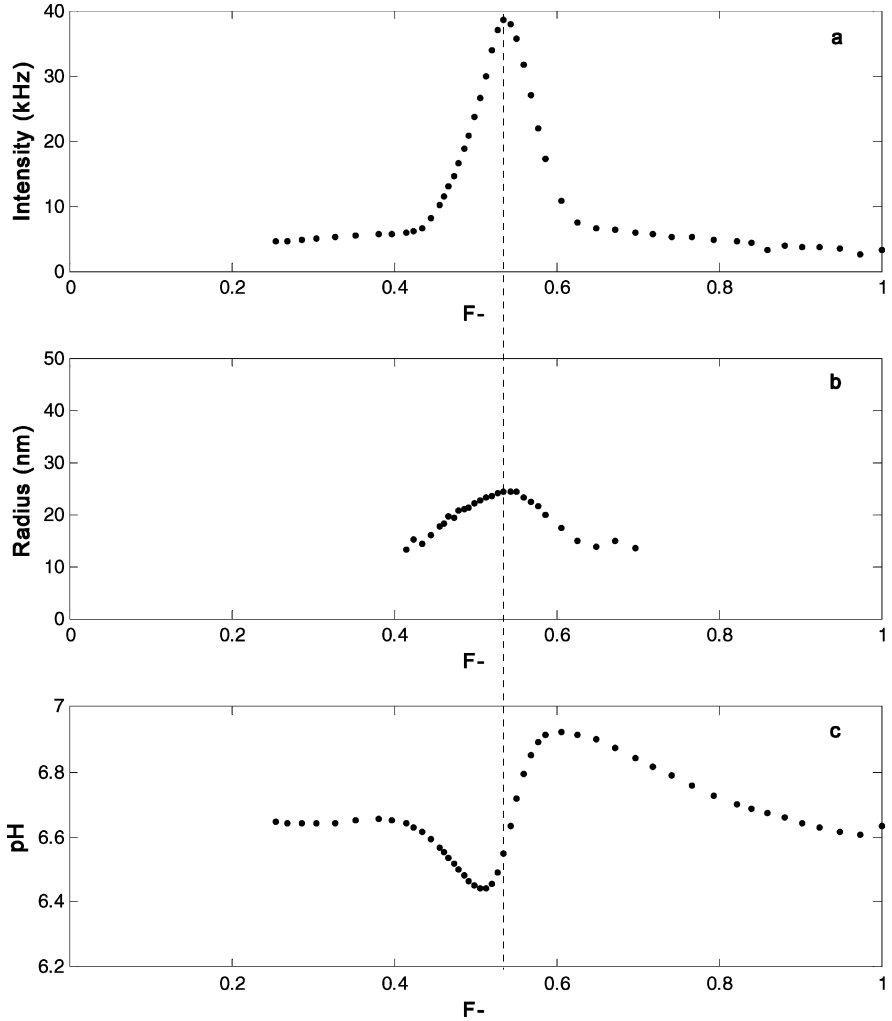

Figure 2. Light-scattering titrations of complex coacervate core micelles made of diblock copolymer and homopolymer: (a) intensity vs composition, (b) hydrodynamic radius vs composition, and (c) pH vs composition. Raw data were provided by Hofs et al.[8]

This is a model-independent way to extract information about the size and shape of the particles.[33−35]

Results and Discussion

Complexation of oppositely charged macromolecules is strongly dependent on the composition of the system. Light-scattering titration is a useful tool to study the complex formation as function of the composition. During a light-scattering titration measurement, charged macromolecules are titrated to a solution with macromolecules of opposite charge. Van der Burgh et al.[7] postulated a diagram of the various species formed due to complexation in such a titration. This diagram is shown in Figure 1. At low F^- positive soluble complexes are formed. Adding more titrant to this solution one arrives at a value of F^- where electroneutral aggregates first appear. These we call "complex coacervate core micelles". At the peak I_{max} in the aggregation diagram these micelles are the dominating species; we call this composition $F^-_{micelle}$. For $F^- > F^-_{micelle}$ overcharging will result in the disintegration of micelles into negatively charged soluble complexes.

In the following section, light-scattering titrations as a function of the composition F^- (eq 1) will be discussed. First we will focus on two-component systems, complexes formed when $PAA_{42}PAAm_{417}$ and $PDMAEMA_{150}$ (Figure 2) or lysozyme and $PAA_{42}PAAm_{417}$ are mixed (Figure 3). Then the three-component systems will be discussed (Figure 4).

Complex Coacervate Core Micelles without Lysozyme. Figure 2 shows the light-scattering titration results for $PAA_{42}PAAm_{417}$ and $PDMAEMA_{150}$ at pH 6.7 and 10 mM $NaNO_3$, taken from Hofs et al.[8] The intensity versus composition curve (Figure 2a) shows a very sharp peak at $F^- \approx 0.5$. The hydrodynamic radius (Figure 2b) at the peak composition ($F^-_{micelle}$) is about 25 nm. The pH versus composition curve (Figure 2c) gives information about the protein uptake and release during the complex formation. The behavior of the pH during the light-scattering titration measurement is rather complicated. This behavior will be discussed in more detail in the section below.

pH during the Light-Scattering Titrations. The change in the proton concentration is due to the proton uptake or release by the macromolecules involved in the complexation process. It gives rise to a typical curve for the pH, shown in Figure 2c. This kind of curve, with pH values that are the same at $F^- = 0$, $F^- = F^-_{micelle}$, and $F^- = 1$, will be found when the pH at which the complexation process is studied is in between the pK's of the different macromolecules.

In our system all the components have a charge that varies with pH. The degree of ionization, α, of these groups can be expressed[36] by eq 2

$$\alpha_{\pm} = \frac{1}{1 + 10^{\pm(\mathrm{pH} - \mathrm{p}K_0 + e\psi)/kT}} \qquad (2)$$

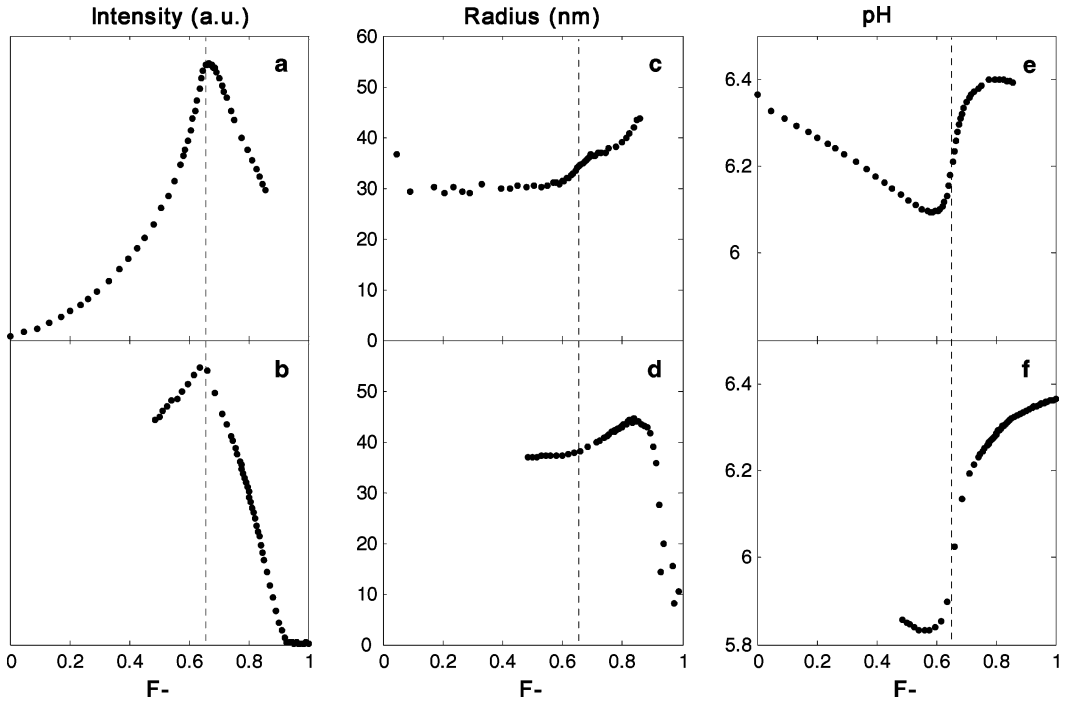

Figure 3. (a) Intensity vs composition (titrating $PAA_{42}PAAm_{417}$ to lysozyme) and **(**b) (titrating lysozyme to $PAA_{42}PAAm_{417}$). **(**c) Hydrodynamic radius vs composition ($PAA_{42}PAAm_{417}$ to lysozyme) and (d) (lysozyme to $PAA_{42}PAAm_{417}$) and (e) pH vs composition ($PAA_{42}PAAm_{417}$ to lysozyme) and **(**f) (lysozyme to $PAA_{42}PAAm_{417}$).

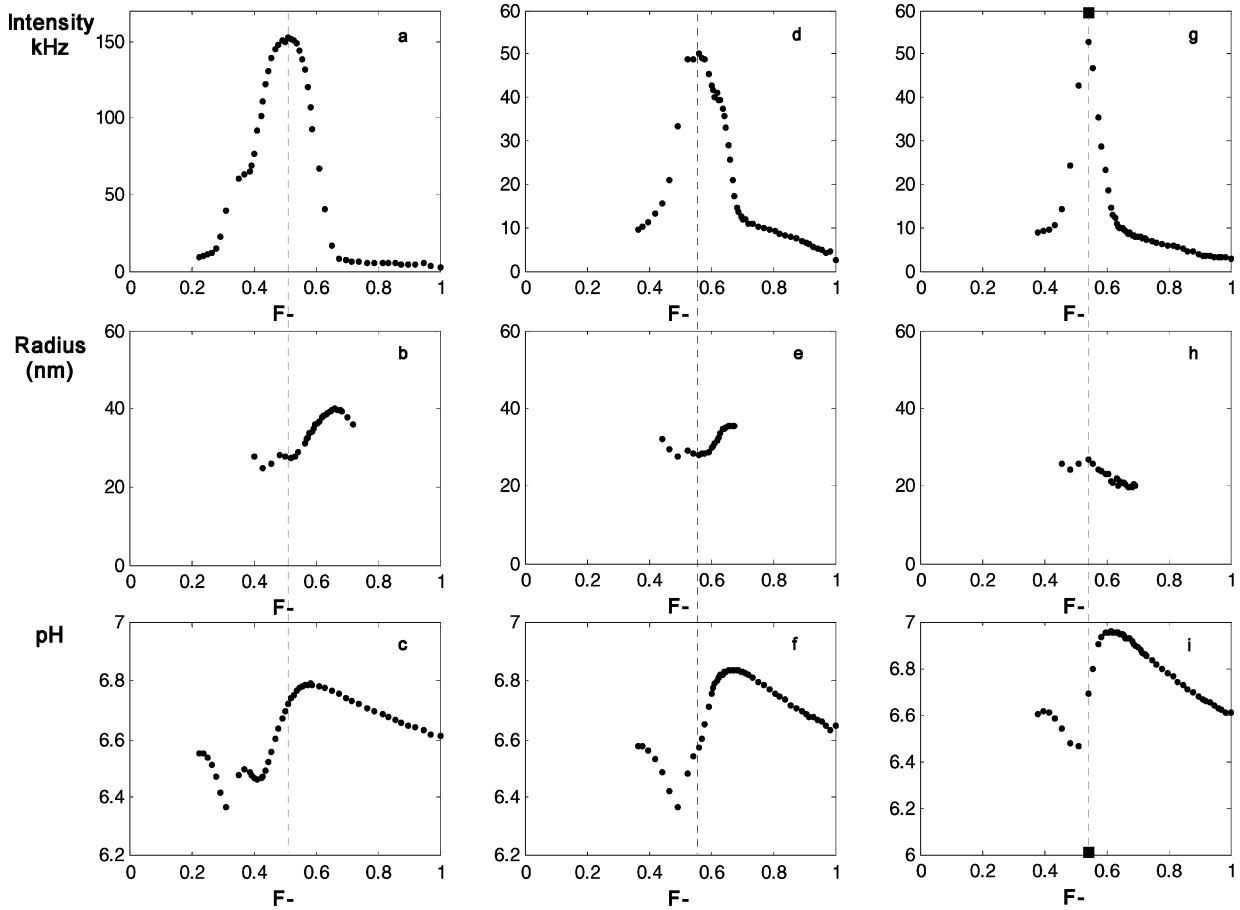

Figure 4. Intensity, hydrodynamic radius, and pH vs composition with three different lysozyme/PDMAEMA molar ratios: (a, b and c) 83:17, (d, e, and f) 3:2, and (g, h, and i) 7:13. In all measurements a mixture of lysozyme and PDMAEMA was added to the $PAA_{42}PAAm_{417}$ solution.

where pH is the measured pH, pK_0 is the intrinsic pK value of the ionizable groups of the macromolecule, Ψ is the electrostatic potential, k is the Boltzmann constant, and T is the temperature.

First consider the extremes of the titration curve. When a positively charged macromolecule is introduced into a solution containing mainly negatively charged macromolecules ($F^- =$

1), the pH increases (Figure 2c). Because the macromolecule experiences a negative potential (eq 2) proton uptake by the polycation is favored. However, protons are released by the polyanion, because the negatively charged macromolecules experience the positive potential of the polycations. Since an increase in pH is measured, it means that the polycation also takes up protons from the solvent. This gives rise to an increase of the pH. At the other extreme of the titration curve, when a negatively charged macromolecule is brought into a solution of mainly positively charged macromolecules ($F^- = 0$), the opposite effect will be seen. Protons are then released, and the bulk pH will decrease.

In the intermediate regime the increasing and decreasing extremes are connected by a curve that crosses the initial pH value. The slope of the curve is steepest at F^-_{micelle} and is actually the "isoelectric point" of the complex; the number of positive charges and negative charges at this composition are the same. Depending on the potential, the negatively charged groups deprotonate, and the positively charged groups protonate. The net effect depends on the differences between the pH and the pK values of the charged groups. For two isolated oppositely charged species, the effect is exactly symmetric for pH values halfway between the two pK's. In that case the extra protonation of the positive species cancels deprotonation of the negative species, and the pH will stay the same. In short, for a symmetric system, at pH $= {}^1/_2(\text{p}K_1 + \text{p}K_2)$, we expect the pH to be the same at $F^- = 0$, $F^- = 0.5$, and $F^- = 1$. If the pH is not the average of the pK's of the system, then the pH curve of a titration experiment can be totally different, but at F^-_{micelle} the slope of the curve is the steepest.

Various complications make a quantitative analysis of these effects rather difficult.[37] In complexes formed by polyelectrolytes or polyampholytes, the effects are not so easy to predict. The potential is already nonzero before complexation, and the potentials felt by groups in the complex are a complicated function of the structure of the complex and the salt concentration. For an amphoteric species, such as a protein, charges may occur in patches. In complexes with such molecules, the distance between attracting charges will be smaller than the distance between repelling charges. The protonation and deprotonation will be complicated in such a system. The titration curve does not just shift but can change in shape as well. Nevertheless, Figure 2c nicely confirms the situation that we have described, because we know that the starting pH in this experiment is pH $= {}^1/_2(\text{p}K_1 + \text{p}K_2)$.

Complex Formation of Lysozyme and $PAA_{42}PAAm_{417}$. Figure 3 shows the results of the light-scattering titrations for the system where all of the homopolymer is replaced by lysozyme. Titrations were performed both by increasing F^- (Figures 3a, 3c, and 3e) as well as by decreasing F^- (Figures 3b, 3d, and 3f).

There is a limited but significant difference between the "up" (increasing F^-) and "down" (decreasing F^-) titrations. Starting with lysozyme in the cuvette (Figures 3a, 3c and 3e), micelles are directly formed. The hydrodynamic radius of these particles is about 30 nm. At $F^- \approx 0.67$ the peak is found. The radius of the particles at this composition is about 37 nm. After the peak (the intensity vs composition), the radius of the particles increases. Since the intensity decreases, the best explanation for this observation is that the aggregates disintegrate partly and become less dense.

The aggregation of the particles in the opposite titration (Figures 3b, 3d, and 3f) follows a different pattern; before micelle formation first soluble complexes are formed. During the first titration steps there is no increase in the light-scattering intensity (Figure 3b). A peak in the intensity versus composition plot is found at the same position as for the diblock copolymer to lysozyme titration. The hydrodynamic radius versus composition (Figure 3d) shows the formation of large structures with a radius of 45 nm at $F^- \approx 0.85$. The size of the particles decreases to about 37 nm; this is the size of the aggregates found at the position of the main peak. The pH versus composition curve for both systems (Figures 3e and 3f) only shows the disintegration of one single type of particle.

Plotting Figures 3a and 3b on top of each other it becomes clear that the formation of the structures is slightly different than the disintegration. It is noticed directly that the curves are asymmetric. When the protein solution is the solution that one starts with (Figure 3a), micelles are directly formed. Similar behavior has been found previously when lysozyme and an oppositely charged chemical analogue of lysozyme are mixed; directly precipitates are formed,[38] and no soluble complexes were formed. Starting from the other side, when the protein solution is the titrant (Figure 3b), first soluble complexes are formed, and only after reaching a certain composition micelles are formed.

Irreversibility of the aggregation process is reflected in the intensity versus composition curves (Figures 3a and 3b) of $F^- = 1$ or $F^- = 0$, respectively; the intensity will be much higher than the starting intensity. A reason for this could be that one diblock copolymer is attached to about five proteins. The electrostatic attraction between diblock copolymer and protein will not be the same for the different protein molecules. For a nonstoichiometric charge ratio this could imply that the proteins that are loosely attached can leave the complex easily, resulting in complexes that are less dense and have a lower light-scattering intensity. These structures have a radius that is the same or larger than that of the original micelles.

A similar system was already studied by Kataoka et al.[15,16] They mixed lysozyme and PEG-p(ASP) at different mixing ratios and determined the size of their complexes with DLS. They never found an asymmetry or irreversibility of their system. A reason that we find this could be that we do not wait long enough after every light-scattering titration step. The system might therefore not be in equilibrium, which is a disadvantage of our measuring method.

However, an advantage of the light-scattering titrations is that the maximal light-scattering intensity indicates at which composition our neutral complexes are formed. In this system F^-_{micelle} is found at 0.67, whereas one would expect to find neutral particles at $F^- = 0.5$ (eq 1). For the calculation of F^- fully charged $PAA_{42}PAAm_{417}$ was taken into account. We know however that the number of charges on this diblock copolymer is pH-dependent. Lysozyme is an amphoteric molecule; the sign and the number of its charges depend on the pH. Therefore we chose to use the titration curve measured by Van der Veen[31] to determine the number of charges at the pH region at which our measurements are performed. The way that we calculate F^- is therefore the reason for this deviation from 0.5. When pH-dependent molecules are involved in complex formation, one should be careful to calculate the composition of the neutral complexes. By using light-scattering titrations, we avoid miscalculations for our neutral complexes, because we can simply determine the composition F^-_{micelle} at $I_{\max}$. This makes it a more accurate way to study these structures than to calculate the stoichiometric composition of the micelles by taking the maximum number of positive charges on the protein molecule.[15,16]

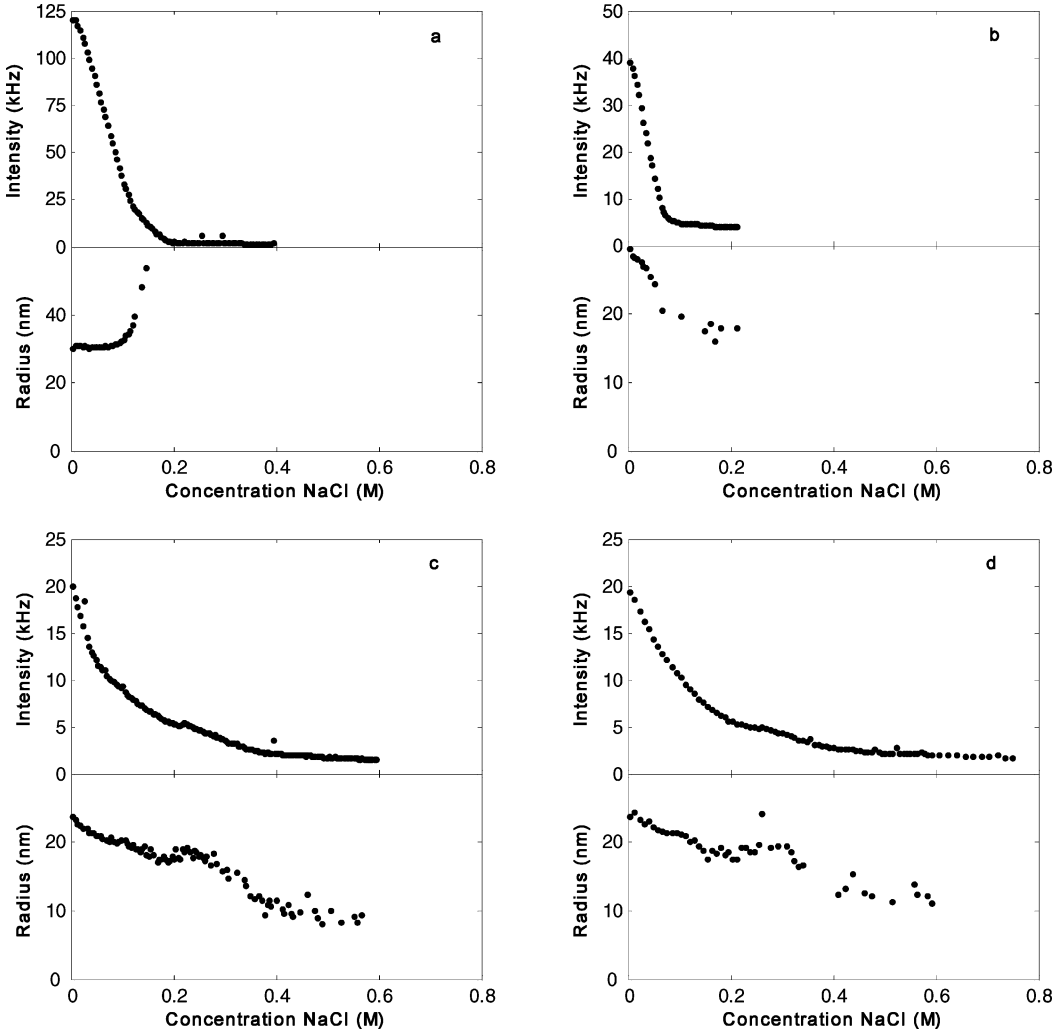

Figure 5. Salt titrations: (a) intensity and radius vs salt concentration for micelles containing only lysozyme, (b) intensity and radius vs salt concentration for 83:17 micelles, (c) intensity and radius vs concentration for 3:2 micelles, and (d) intensity and radius vs concentration for 7:13 micelles.

Complex Formation at Different Lysozyme/PDMAEMA Ratios. Figure 4 contains the light-scattering titration results for three different systems with different lysozyme to PDMAEMA$_{150}$ molar ratios: 83:17, 3:2, and 7:13. The curves in Figures 4a, 4d, and 4g show the intensity as function of the composition F^- (eq 1). In Figures 4b, 4e, and, 4h the radius of the particles that are formed during the titrations can be found. In Figures 4c, 4f, and 4i the pH of the solution during the measurement is plotted. The data are individually discussed for the three different systems.

In Figure 4a it is seen that $F^-_{\text{micelle}} \approx 0.5$. Particles at this composition have a hydrodynamic radius of about 28 nm (Figure 4b). In the intensity versus composition curve a shoulder is found at $F^- \approx 0.4$, suggesting the formation of another structure with a radius of about 25 nm. The same was observed starting at $F^- = 0$ (results not shown). A possible explanation for this phenomenon is that the attraction between the homopolymer and the diblock copolymer is stronger than the attraction between the diblock copolymer and the protein, because of the difference in charge density between the homopolymer and the lysozyme molecule. Therefore the homopolymer will be preferably taken up in the micelles, and when a small amount of positively charged components is needed (low F^- value) lysozyme will be expelled from the complexes. The new particles that are formed contain a lower lysozyme to PDMAEMA ratio. Those complexes are expected to have a lower light-scattering intensity and a smaller radius. This observation is confirmed by the pH versus composition curves.

Because the intensity, hydrodynamic radius, and pH as function of the composition all suggest the formation of a second particle, we tried to analyze the light-scattering autocorrelation functions more extensively. Both biexponential fitting these curves and a CONTIN analysis did not give indications of multiple species being present at the same time. The concentration of individual protein molecules is too low to be determined using light scattering.

Like the system where lysozyme is in excess (Figures 4a−c), the 3:2 system also seems to have a shoulder at $F^- \approx 0.62$. The radius versus composition curve (Figure 4e) shows that in this system most likely another particle is formed. The particle formed at F^-_{micelle} has a hydrodynamic radius of about 28 nm; the second particle has a hydrodynamic radius of about 35 nm. In the pH versus composition plot (Figure 4f) only a small kink is seen, which could correspond to the formation of this second particle as well.

The last system considered is the system where the positively charged component predominantly consists of homopolymer (Figures 4g−i). One single sharp peak at $F^- \approx 0.56$ is found in the intensity versus composition plot. The formation of one type of particle is confirmed by the hydrodynamic radius versus composition and the pH versus composition plots. These results strongly resemble the results of the light-scattering titration of

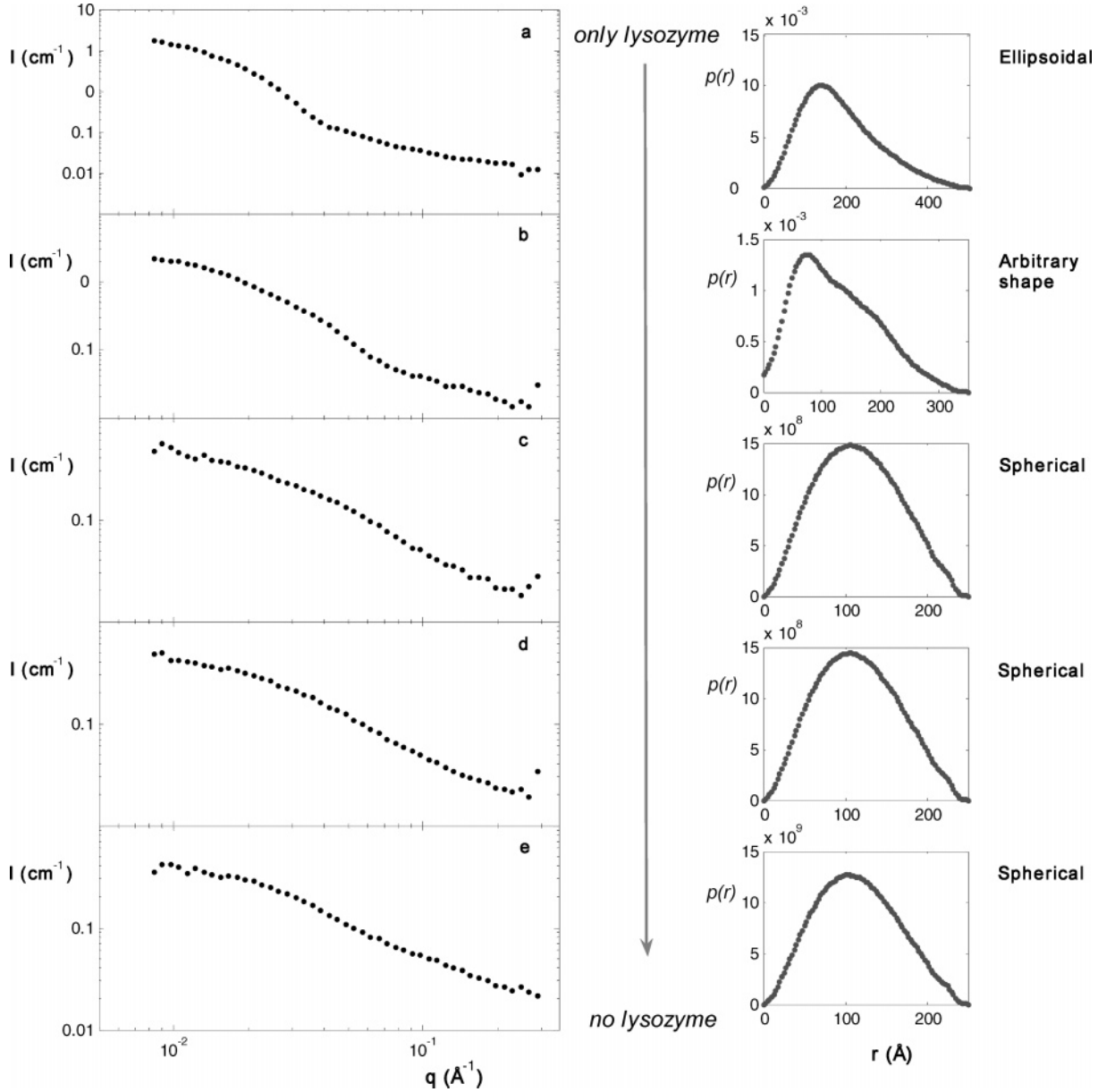

Figure 6. Neutron-scattering intensity (*I*) curves as function of scattering vector *q* for the five different systems. From a to e the ratios between lysozyme/homopolymer are 1:0, 83:17, 3:2, 7:13, and 0:1, respectively. The corresponding pair distance distribution functions as function of *r* (in Å) for these systems are plotted on the right side.

the homopolymer to the diblock copolymer (Figure 2). The radius of the particles formed at the composition of the peak is about 22 nm.

Summarizing the light-scattering titrations, we can say that the broader intensity versus composition curves are obtained at higher lysozyme to homopolymer ratios. When lysozyme is in excess more than one type of particle seems to be formed, but these structures might not exist simultaneously. The system predominantly consisting of homopolymer shows only one kind of micelle.

Titrations with NaCl Solution. Since electrostatics is the main driving force of the complex formation, the stability of the complexes will depend on the ionic strength. Therefore a second type of light-scattering titration was performed to determine the resistance of the micelles toward salt. Solutions with composition F^{-}_{micelle} were prepared, and a 4 M NaCl solution was titrated to these solutions. The intensity and the radius as a function of NaCl concentration are shown in Figure 5 for the four different systems studied.

For all of the systems the intensity as function of the salt concentration decreases. This is to be expected since the electrostatic interactions become weaker when the salt concentration is increased due to screening of the charges. The particles are expected to swell when salt is added, resulting in larger radii. Salt resistance is markedly different for the different systems. For micelles containing only lysozyme (Figure 5a), the salt concentration at which the particles fall apart can accurately be determined. At 0.12 M NaCl the radius of these complex coacervate core micelles is increasing. The error at higher salt concentrations is very largely increased compared to the error at lower salt concentrations.

For the micelles predominantly consisting of lysozyme (Figure 5b), the intensity as function of the salt concentration drops off much steeper than that for the system with only lysozyme. The radius as function of the salt concentration decreases. The error in the radius does not increase as much as for the micelles containing only lysozyme. A possible explanation could be that the proteins are expelled from the micelles

and complexes of homopolymer and diblock copolymer are favored. These complexes are expected to have a smaller radius and have a lower light-scattering intensity.

Figures 5c and 5d are very much alike. The salt resistance of the micelles predominantly consisting of homopolymer (Figure 4c) seems to be slightly better than the salt resistance of the 3:2 system (Figure 5c). In summary, the results in Figure 5 show that the salt resistance increases when the cores of the complex coacervate core micelles contain more homopolymer. For micelles with mixed cores it seems that at a certain salt concentration lysozyme seems to be expelled from this core. The particles that are formed then have smaller radii.

It is known that the number of charges and the charge density on the molecules that are participating are relevant parameters in complex formation.[7] For instance, complex coacervate core micelles made of oppositely charged block copolymers are less salt resistant than complex coacervate core micelles made of a diblock copolymer and oppositely charged homopolymer.[8] Therefore it is not surprising that the structures made of protein and diblock copolymers are more sensitive to increases of the ionic strength than the complexes with mixed cores.

Small-Angle Neutron Scattering. From the dynamic light-scattering titration measurements we know the hydrodynamic radius of the complex coacervate core micelles, but we are also interested in the structure and composition of the core. A method to obtain this information is SANS. The relatively densely packed cores of the micelles have a much higher contrast with the surrounding medium than the dilute corona. Figure 6 shows the scattering curves of five different systems with different amounts of lysozyme in the cores. The first remark about the scattering curves is that no distinct minima are observed. If the micellar cores had been monodisperse, then, given the instrument setup, we would certainly have been able to observe form factor minima.

Unfortunately, for the present data the q-range does not extend to low enough q-values ($qR \ll 1$) such that we could do a Guinier analysis to extract the radii of gyration and to extrapolate to $q = 0$ to obtain the core contrast, which should be indicative of the water content. Also, form factors of homogeneous spheres fit very poorly, presumably because the core inhomogeneities contribute significantly to the scattering at higher q.[39]

Therefore, instead we have used the GIFT method. This method gives a model-free representation of the scattering data, which is called the pair distance distribution function (PDDF), $p(r)$. Even for inhomogeneous particles the $p(r)$ function is proportional to the number of pairs of electrons separated by the distance r. This is the distance that is found in combination of any volume element i with any volume element k of the same particle. The shape of the $p(r)$ function gives an indication about the shape of the particles.[33−35]

The scattering curves of the different systems are clearly different. The micelles containing only protein have a high scattering intensity at low q compared to those of the other systems. The function $p(r)$ of this system tells us that the shape of the cores of these types of micelles is most likely ellipsoidal.[35] The pair distance distribution function of micelles predominantly consisting of lysozyme does not indicate a well-defined structure. Light-scattering titrations for this system as function of the composition and the salt titration already showed the presence of a second particle. Comparing the $p(r)$ function to the $p(r)$ functions of the other systems, one could say that it seems to be an intermediate between the $p(r)$ of an ellipsoid and a sphere. The $p(r)$ function of the average scattering curve of the micelles with only lysozyme and the micelles with only homopolymer does not give a similar pair distance distribution function.

The last three scattering curves for the systems with lysozyme/homopolymer ratios of 3:2 and 7:13 and the complex coacervate core micelles made of homopolymer only are quite similar. The pair distance distribution functions of these systems show that the shape of the structures is spherical. The radius of the spheres is however much smaller than the hydrodynamic radius measured with light scattering. This suggests that the core scattering dominates.

At high q the intensity in the scattering curves of the complex coacervate core micelles with proteins (Figures 6b, 6c, and 6d) seems to increase whereas a curve without protein (Figure 6e) decreases. This could be an indication that at higher q it should be possible to find a structure peak of the protein molecules. Berret et al. found structure peaks of micelles in the neutron-scattering curves of core−shell structures made of micelles and oppositely charged diblock copolymers.[39] This structure peak is found at $q > 0.15$ Å^{-1}, which is within the q-range of our neutron-scattering experiment, but the micelles that Berret used were larger than our protein molecules. It would be worthwhile for a next SANS experiment to go to higher q and try to find out whether this increase in intensity is caused by the structure peak of the protein molecules.

From the SANS data we tried to determine the number of proteins inside the cores of our micelles. In the absence of a more precise determination by fitting the SANS data over much wider q-range, we here estimate the number of proteins inside the cores of the micelles based on the results of the GIFT anaylysis. As a first estimation of the number of lysozyme molecules in the core of the spherical complexes, we use the radius of the sphere (the top of the PDDF) to calculate the total volume of the micelles. Since we know the composition of the complexes and we know the radius of the proteins, we can calculate the number of lysozyme molecules. For the 3:2 system this is about 38, and for the 7:13 system this results in 15 lysozyme molecules per micelle.

The number calculated in this way would only be correct if there were not any water in the cores of the complexes. Since it is known that complex coacervates contain a large fraction of water, the actual number of proteins in the cores is expected to be lower. Weinbreck et al.[5] determined the amount of water by freeze-drying the complex coacervate phase. They determined for their system that the water content was about 67%. If we now correct the calculated numbers using this information, then this would mean that for the 3:2 micelles the number of enzymes inside the core is about 13, and for the 7:13 micelles this would result in 5 protein molecules per core.

Conclusions

We have shown the possibility to encapsulate proteins in complex coacervate core micelles. We are able to control the number of lysozyme molecules in the cores of the micelles by changing the mixing ratio between lysozyme and the like-charged homopolymer. The shape and stability of these micelles also depend on this mixing ratio. The most stable micelles are formed when homopolymer is in excess over lysozyme. The estimated number of protein molecules in the cores of these micelles is 5−15. This suggests that the enzymes in the core are accessible, which would make them suitable for enzymatic applications.

Acknowledgment. We thank Richard Heenan for his assistance with the SANS experiments and Otto Glatter for the

CDV

useful discussions and explanation of the GIFT software. We also thank Bas Hofs for the raw data in Figure 2. This work has been financed by the NWO (Dutch Scientific Research Foundation).

References and Notes

(1) Bungenberg de Jong, H. G. In *Colloid Science*; Kruyt, H. R., Ed.; Elsevier: Amsterdam, 1949; Vol. 2, pp 335−432.
(2) Gibbs, B. F.; Kermasha, S.; Alli, I.; Mulligan, C. N. *Int. J. Food Sci. Nutr.* **1999**, *50*, 213−224.
(3) Kataoka, K.; Harada, A.; Nagasaki, Y. *Adv. Drug Delivery Rev.* **2001**, *47*, 113−131.
(4) Schmitt, C.; Sanchez, C.; Desobry-Banon, S.; Hardy, J. *Crit. Rev. Food Sci. Nutr.* **1998**, *38*, 689−753.
(5) Weinbreck, F.; Wientjes, R. H. W. *J. Rheol.* **2004**, *48*, 1215−1228.
(6) de Kruif, C. G.; Weinbreck, F.; de Vries, R. *Curr. Opin. Colloid Interface Sci.* **2004**, *9*, 340−349.
(7) van der Burgh, S.; de Keizer, A.; Stuart, M. A. C. *Langmuir* **2004**, *20*, 1073−1084.
(8) Hofs, B.; Voets, I. K.; Keizer, A. d.; Cohen Stuart, M. A. *Phys. Chem. Chem. Phys.* **2006**, *8*, 4242−4251.
(9) Voets, I. K.; de Keizer, A.; Stuart, M. A. C.; de Waard, P. *Macromolecules* **2006**, *39*, 5952−5955.
(10) Voets, I. K.; de Keizer, A.; de Waard, P.; Frederik, P. M.; Bomans, P. H. H.; Schmalz, H.; Walther, A.; King, S. M.; Leermakers, F. A. M.; Stuart, M. A. C. *Angew. Chem., Int. Ed.* **2006**, *45*, 6673−6676.
(11) Stuart, M. A. C.; Besseling, N. A. M.; Fokkink, R. G. *Langmuir* **1998**, *14*, 6846−6849.
(12) Harada, A.; Kataoka, K. *Macromolecules* **1995**, *28*, 5294−5299.
(13) Kabanov, A. V.; Bronich, T. K.; Kabanov, V. A.; Yu, K.; Eisenberg, A. *Macromolecules* **1996**, *29*, 6797−6802.
(14) van der Burgh, S.; Fokkink, R.; de Keizer, A.; Stuart, M. A. C. *Colloids Surf., A* **2004**, *242*, 167−174.
(15) Harada, A.; Kataoka, K. *Macromolecules* **1998**, *31*, 288−294.
(16) Harada, A.; Kataoka, K. *Langmuir* **1999**, *15*, 4208−4212.
(17) Harada, A.; Kataoka, K. *Abstr. Pap. Am. Chem. Soc.* **2000**, *219*, U458.
(18) Harada, A.; Kataoka, K. *J. Controlled Release* **2001**, *72*, 85−91.
(19) Harada, A.; Kataoka, K. *J. Am. Chem. Soc.* **2003**, *125*, 15306−15307.
(20) Yuan, X. F.; Harada, A.; Yamasaki, Y.; Kataoka, K. *Langmuir* **2005**, *21*, 2668−2674.
(21) Yuan, X. F.; Yamasaki, Y.; Harada, A.; Kataoka, K. *Polymer* **2005**, *46*, 7749−7758.
(22) Wakebayashi, D.; Nishiyama, N.; Itaka, K.; Miyata, K.; Yamasaki, Y.; Harada, A.; Koyama, H.; Nagasaki, Y.; Kataoka, K. *Biomacromolecules* **2004**, *5*, 2128−2136.
(23) Wakebayashi, D.; Nishiyama, N.; Yamasaki, Y.; Itaka, K.; Kanayama, N.; Harada, A.; Nagasaki, Y.; Kataoka, K. *J. Controlled Release* **2004**, *95*, 653−664.
(24) Jaturanpinyo, M.; Harada, A.; Yuan, X. F.; Kataoka, K. *Bioconjugate Chem.* **2004**, *15*, 344−348.
(25) Berret, J.-F. *J. Chem. Phys.* **2005**, *123*, 164703.
(26) Berret, J.-F.; Schonbeck, N.; Gazeau, F.; El Kharrat, D.; Sandre, O.; Vacher, A.; Airiau, M. *J. Am. Chem. Soc.* **2006**, *128*, 1755−1761.
(27) Berret, J.-F.; Sehgal, A.; Morvan, M.; Sandre, O.; Vacher, A.; Airiau, M. *J. Colloid Interface Sci.* **2006**, *303*, 315−318.
(28) Berret, J.-F.; Yokota, K.; Morvan, M. *Soft Mater.* **2004**, *2*, 71−84.
(29) Taton, D.; Wilczewska, A. Z.; Destarac, M. *Macromol. Rapid Commun.* **2001**, *22*, 1497−1503.
(30) Chalikian, T. V.; Totrov, M.; Abagyan, R.; Breslauer, K. J. *J. Mol. Biol.* **1996**, *260*, 588−603.
(31) van der Veen, M.; Norde, W.; Stuart, M. C. *Colloids Surf., B* **2004**, *35*, 33−40.
(32) Salomaa, P.; Schaleger, L. L.; Long, F. A. *J. Am. Chem. Soc.* **1964**, *86*, 1−7.
(33) Glatter, O. *J. Appl. Crystallogr.* **1977**, *10*, 415−421.
(34) Glatter, O. *J. Appl. Crystallogr.* **1979**, *12*, 166−175.
(35) Glatter, O.; Kratky, O. *Small Angle X-ray Scattering*; Academic Press: London, 1982.
(36) Biesheuvel, P. M.; Stuart, M. A. C. *Langmuir* **2004**, *20*, 2785−2791.
(37) Ullner, M.; Jonsson, B. *Macromolecules* **1996**, *29*, 6645−6655.
(38) Biesheuvel, P. M.; Lindhoud, S.; de Vries, R.; Stuart, M. A. C. *Langmuir* **2006**, *22*, 1291−1300.
(39) Berret, J. F.; Herve, P.; Aguerre-Chariol, O.; Oberdisse, J. *J. Phys. Chem. B* **2003**, *107*, 8111−8118.

BM0700688